Int. J. Exp. Path. (1993) **74**, 103–112

Production of salivary microlithiasis in cats by parasympathectomy: light and electron microscopy

A. TRIANTAFYLLOU, J.D. HARRISON AND J.R. GARRETT
Department of Oral Pathology, King's College School of Medicine and Dentistry, London, UK

Received for publication 17 July 1992
Accepted for publication 5 November 1992

Summary. Salivary glands of cat were examined from 1 to 42 days following parasympathectomy and compared with contralateral normal control glands. Microliths were detected by light microscopy in none of 11 parotid, 31 out of 41 submandibular and four out of 22 sublingual glands following parasympathectomy, and one out of 19 parotid, five out of 28 submandibular and four out of 15 sublingual normal control glands. The greatly increased occurrence of microliths in the submandibular gland was statistically significant. Microliths in the parasympathectomized submandibular glands were detected by light microscopy most often in ductal lumina, followed by acinar lumina, ductal parenchyma, interstitial stroma, and acinar parenchyma. They were detected by electron microscopy also in the basement membrane overlying protruding processes of myoepithelial cells and in intraparenchymal macrophages. Intracellular microliths were in phagosomes. In the parasympathectomized submandibular glands, parenchymal atrophy was seen and particularly involved the striated ducts; secretory material and cellular debris were seen in lumina; and macrophages and neutrophils were more apparent than normally. The great increase of microlithiasis in the submandibular gland appears to be the result of secretory inactivity, and microliths appear to form in stagnant secretory material and cellular debris in lumina and in phagosomes of parenchymal cells.

Keywords: calcinosis, calculi, denervation, microlithiasis, salivary glands, sialadenitis

Although microliths occur in human salivary glands and may be of aetiological significance in chronic sialadenitis and sialolithiasis (Tandler 1965; Seifert & Donath 1977; Scott 1978; Epivatianos *et al*. 1987; Epivatianos & Harrison 1989; Harrison & Epivatianos 1992), little is known about the factors responsible for the production of microliths themselves. However, secretory inactivity has been suggested as a factor (Epivatianos & Harrison 1989), and so we decided to investigate this in feline salivary glands, in which microliths occur normally (Epivatianos *et al*. 1986; Triantafyllou 1991). Saliva is produced by parasympathetic and sympathetic impulses, of which the former is responsible for most of the saliva in the cat (Emmelin 1953; Garrett & Kidd 1975; Emmelin & Garrett 1989), and an archival collection of denervated feline salivary glands was fortunately available.

Correspondence: Dr J.D. Harrison, Department of Oral Pathology, The Rayne Institute, 123 Coldharbour Lane, London SE5 9NU, U.K.

Materials and methods

Animals and glands

Archival salivary glands from 40 mature cats were used

Table 1. Occurrence of microliths detected light microscopically in wax-embedded pieces of salivary glands of cat

Gland	Glands from which pieces taken	Glands in which microliths detected
Control		
Parotid	19	1
Submandibular	28	5
Sublingual	15	4
Parasympathectomized		
Parotid	11	0
Submandibular	41	31
Sublingual	22	4
Parasympathectomized and sympathectomized		
Parotid	0	0
Submandibular	4	2
Sublingual	4	1

and had been prepared as described by Garrett (1966*a*, *b*), Garrett and Kidd (1975) and Edwards and Garrett (1988): glands subjected to parasympathectomy for periods from 1 to 42 days; glands subjected to combined parasympathectomy and sympathectomy for periods from 1 to 35 days; and contralateral normal control glands (Table 1). Parasympathectomized glands included 14 (nine submandibular, five sublingual) that had received sympathetic nerve stimulation during the terminal part of the experiment.

Avulsion of the auriculotemporal nerve had effected parotid post-ganglionic parasympathectomy, and excision of the chorda tympani had effected submandibular preganglionic and partial post-ganglionic parasympathectomy. Avulsion of the superior cervical ganglion had effected sympathectomy. Electrical stimulation of the cervical sympathetic trunk had effected sympathetic nerve stimulation. The animals had been fasted overnight before the procedures. The denervations had been effected during anaesthesia with pentobarbitone (36 mg/kg i.p.), and the removal of the glands during similar anaesthesia, except following the stimulations, for which the animals had been anaesthetized with chloralose (70 mg/kg i.p.) following induction with chloroform or ether. The experiments had been terminated with an overdose after the removal of the glands.

Preservation

For histology, pieces of gland had been fixed overnight in formaldehyde–sucrose as described by Garrett and Kidd (1975), Lillie's formaldehyde–calcium (Lillie 1965), or occasionally in Carnoy, formaldehyde–Zenker or Bouin fixative (Lillie 1965), or glands had been perfusion fixed by a solution of glutaraldehyde and formaldehyde as described by Garrett and Kidd (1975). Pieces of greatest dimension of no more than 1 cm had finally been embedded in paraffin wax.

For electron microscopy, immersion or perfusion fixation had been used as described by Garrett and Kidd (1975). Immersion fixation had been in solutions of: glutaraldehyde and formaldehyde, which occasionally also contained acrolein; glutaraldehyde; or osmium tetroxide. Perfusion had been by a solution of glutaraldehyde and formaldehyde. Pieces fixed by aldehydes had been subsequently post-fixed in osmium tetroxide. Pieces of greatest dimension of less than 2 mm had finally been embedded in Araldite.

Microscopy

For light microscopy, sections of the wax-embedded pieces were stained with haematoxylin and eosin.

For electron microscopy, sections of Araldite-embed-

Table 2. Localization of microliths detected light microscopically in wax-embedded pieces of salivary glands of cat

		Submandibular			Sublingual		
Localization	Parotid Control	Control	Para-sympathectomized	Parasympathectomized and sympathectomized	Control	Para-sympathectomized	Parasympathectomized and sympathectomized
Acinar parenchyma	0	1	38	1	2	0	6
Ductal parenchyma	0	2	163	0	1	0	0
Acinar lumina	0	1	192	2	1	1	1
Ductal lumina	1	7	833	0	0	0	0
Interstitial stroma	0	1	62	2	3	4	3
Total	1	12	1288	5	7	5	10

Table 3. Localization of microliths detected light microscopically in wax-embedded pieces of parasympathectomized submandibular glands of cat at different durations

Localization	Days after parasympathectomy													Total
	2	4	5	8	14	16	21	22	24	28	32	35	42	
Acinar parenchyma	0	0	0	30 (1)	2 (2)	0	3 (3)	2 (1)	1 (1)	0	0	0	0	38 (8)
Ductal parenchyma	0	0	0	0	7 (2)	1 (1)	33 (6)	19 (3)	52 (4)	6 (1)	39 (1)	1 (1)	5 (1)	163 (20)
Acinar lumina	0	0	0	180 (1)	2 (1)	0	6 (4)	2 (1)	2 (1)	0	0	0	0	192 (8)
Ductal lumina	1 (1)	30 (2)	15 (1)	26 (2)	175 (5)	16 (1)	156 (8)	58 (3)	259 (4)	43 (1)	41 (1)	4 (1)	9 (1)	833 (31)
Interstitial stroma	0	0	0	0	1 (1)	1 (1)	0	1 (1)	13 (3)	13 (1)	29 (1)	0	4 (1)	62 (9)
Total	1 (1)	30 (2)	15 (1)	236 (2)	187 (5)	18 (1)	198 (8)	82 (3)	327 (4)	62 (1)	109 (1)	5 (1)	18 (1)	1288 (31)

The numbers in parentheses following the numbers of microliths indicate the numbers of glands in which the microliths were detected.

ded pieces were obtained from a submandibular and a parotid control gland and 18 submandibular glands and 1 sublingual gland parasympathectomized for periods from 1 to 32 days, and included all the glands in which the highest numbers of microliths in the wax-embedded pieces were detected. Parasympathectomized submandibular glands included seven that had received sympathetic nerve stimulation during the terminal part of the experiment. Semithin sections for light microscopical orientation were stained with Methylene Blue and Azure II followed by Basic Fuchsin (Humphrey & Pittman 1974), which has been previously used in investigations of calcified material (Rees & Ali 1988). Ultrathin sections for electron microscopy were stained with lead citrate (Reynolds 1963).

Table 4. Localization of sites of microliths detected electron microscopically in parasympathectomized submandibular glands of cat

Localization	Sites of microliths
Central acinar cells	32
Demilunar acinar cells	1
Myoepithelial cells	2
Ductal cells	47
Unidentified cells in parenchyma	21
Parenchymal intercellular spaces	1
Acinar lumina	60
Ductal lumina	125
Acinar basement membrane	56
Macrophages in acinar parenchyma	12
Macrophages in ductal parenchyma	24
Macrophages in acinar lumina	1
Neutrophils in ductal parenchyma	2
Total	384

Statistics

Differences between the numbers of parasympathectomized and control glands in which microliths were detected in wax-embedded pieces (Table 1) were tested by the χ^2-test for fourfold tables with Yates's correction (Bailey 1981).

Results

Light microscopy of wax-embedded pieces

The occurrence of microliths detected in wax-embedded pieces is shown in Table 1. The difference between the occurrence of microliths in parasympathectomized and control submandibular glands was statistically significant at the 1% level ($\chi^2 = 19.98$, for one degree of freedom), whereas the differences between parasympathectomized and control parotid ($\chi^2 = 0.08$) and sublingual ($\chi^2 = 0.04$) glands were not significant for one degree of freedom. Seven out of the 31 parasympathectomized submandibular glands in which microliths were detected (Table 1) had received sympathetic nerve stimulation during the terminal part of the experiment.

The localization of microliths is shown in Table 2. There was a greatly increased occurrence in the parasympathectomized submandibular glands, in which the localization of microliths at the different durations following parasympathectomy is shown in Table 3.

Parenchymal atrophy was seen in the denervated submandibular glands from 4 days and mainly involved

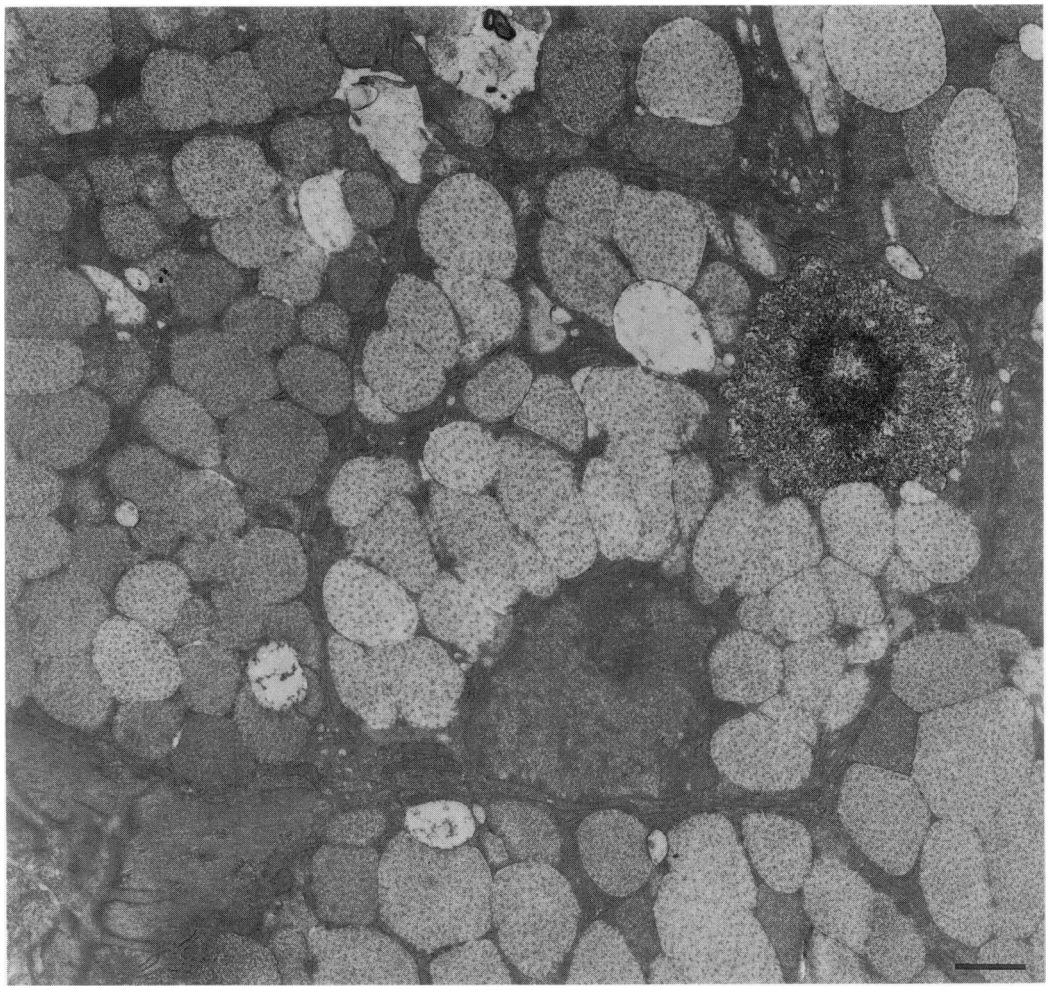

Figure 1. Submandibular gland 24 days after parasympathectomy. Perfusion fixed in glutaraldehyde and formaldehyde, and subsequently immersion fixed in osmium tetroxide. A microlith that consists of a high concentration of crystals is present in an autophagosome situated in the top right of one of the central acinar cells that surround a small lumen and are filled with secretory granules. Part of a myoepithelial cell is seen in the lower left and small processes protrude stromally. ×9100; bar 1 μm.

the striated ducts, although acinar atrophy was seen. Acinar atrophy was seen in the denervated sublingual glands, whereas the denervated parotid glands appeared similar to the controls. Increased numbers of inflammatory cells were seen in the denervated submandibular and sublingual glands from 4 days and were most evident in the submandibular glands. The appearance of the control glands was similar to that of previously described normal glands (Shackleford & Wilborn 1970; Tandler & Poulsen 1977; König & Kühnel 1986).

Electron microscopy of Araldite-embedded pieces

Microliths were detected electron microscopically in 15 parasympathectomized submandibular glands. The localization and appearance of the microliths is shown in Table 4 and Figures 1–6. The microliths in the acinar parenchyma and lumina varied in their greatest dimension of section profile measured on electron micrographic prints from 0.5 to 16.0 μm, those in the ductal parenchyma from 0.4 to 28.3 μm and those in the ductal lumina from 0.5 to 36.6 μm. Forty-four of the 47 microliths detected in ductal cells were situated in large ducts (Figure 2) and the other three in identifiable intercalary ducts. The intracellular microliths were in phagosomes (Figures 1, 2 and 6). The microliths in the acinar basement membrane measured from 0.5 to 1.5 μm, and were detected only around processes of myoepithelial

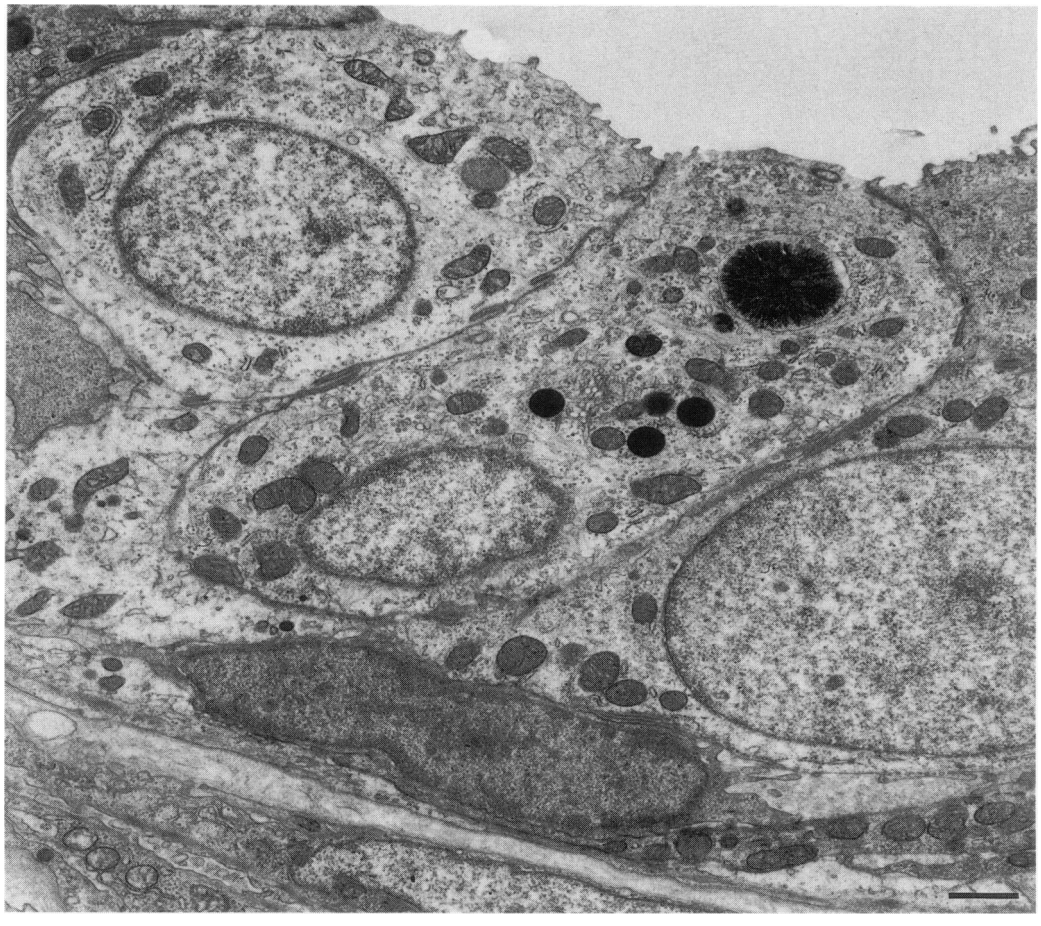

Figure 2. Submandibular gland 4 days after parasympathectomy. Immersion fixed in osmium tetroxide. One of the cells of a large intralobular duct contains a microlith in a phagosome situated luminally, and a group of electron-dense lysosomes between it and the nucleus. ×9100; bar 1 μm.

cells that protruded into the stroma (Figure 5). The microliths consisted of crystals, and granular material that was particularly evident in those in ductal lumina (Figure 4). They sometimes appeared to be arranged in groups, and showed evidence of growth and fusion by accretion. Therefore, each group was counted as one site when assessing microliths electron microscopically (Table 4), in order to avoid bias such as could be caused by counting the two groups of microliths in Figure 5 as many sites.

The localization of microliths in the parasympathectomized glands that had been sympathetically stimulated was similar to that in the unstimulated glands.

The parasympathectomized submandibular glands showed a variable atrophy from 4 days. The striated ducts showed the greatest changes, which included a variable loss of the basal infoldings of the plasma membrane and associated concentrations of mitochondria, an increased proportion of basal cells, and a variable loss of the apical secretory granules, which were absent after sympathetic stimulation. Atrophic striated ducts were often indistinguishable from excretory ducts, and so together they were called large ducts (Figures 2, 4 and 6). Atrophic central acinar cells were seen, and showed a variable loss of secretory granules. Demilunar acinar cells showed a loss of secretory granules following sympathetic stimulation. Myoepithelial cells were more conspicuous than normal and small processes that protruded stromally were seen (Figures 1 and 5). Thickening of the basement membrane was seen (Figure 5). Autophagosomes containing secretory granules were seen in central acinar cells, and phagosomes in large ductal cells. Secretory material, cellular debris, macrophages and neutrophils were seen in lumina, and

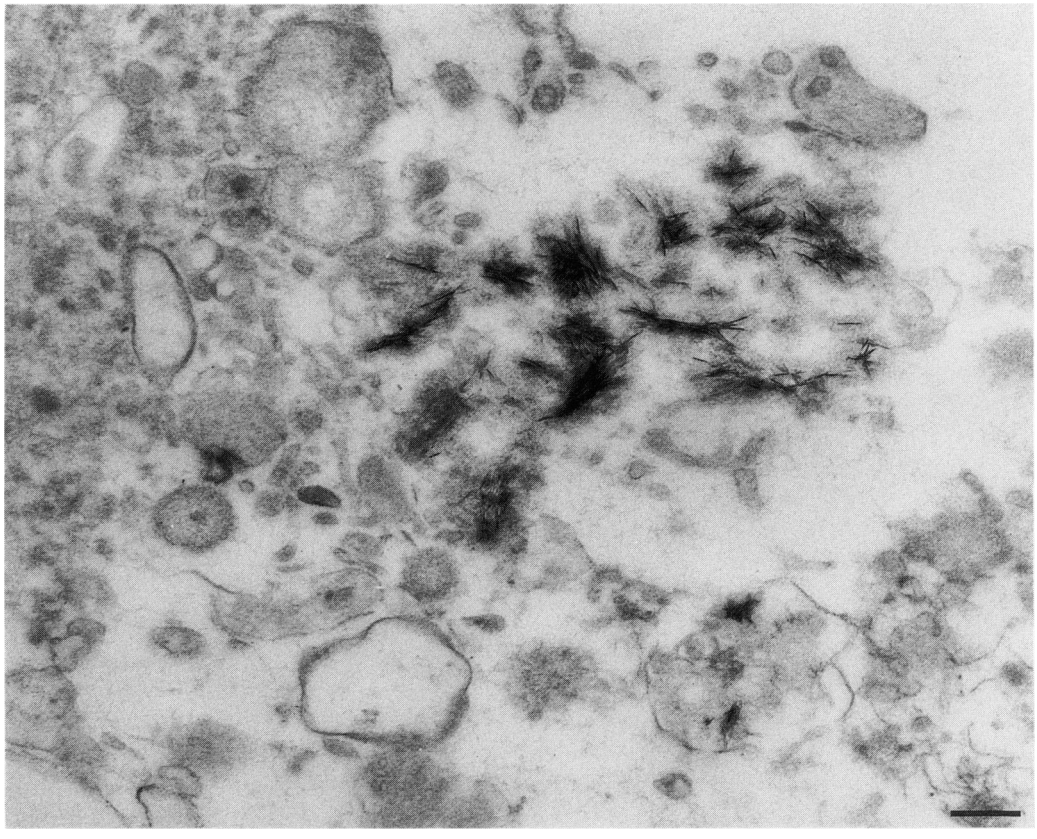

Figure 3. Submandibular gland 24 days after parasympathectomy. Immersion fixed in glutaraldehyde and formaldehyde, and subsequently in osmium tetroxide. Part of the lumen of a large intralobular duct contains clusters of needle-shaped crystals associated with secretory material and cellular debris. × 45400; bar 0.2 μm.

the inflammatory cells were seen between parenchymal cells and in the stroma (Figures 3, 4 and 6).

The appearance of the control glands was similar to that of previously described normal glands (Shackleford & Wilborn 1970; König & Kühnel 1986).

Discussion

The finding that parasympathectomy is followed by a greatly increased occurrence of microliths in the submandibular gland of cat supports the suggestion that secretory inactivity is an important aetiological factor of salivary microlithiasis. This increase contrasts with the absence of microliths in the parasympathectomized parotid glands and the lack of any increase in the parasympathectomized sublingual glands. However, the parotid gland is supplied by parasympathetic fibres other than those in the auriculotemporal nerve that are sufficient to maintain secretory activity after section of the auriculotemporal nerve and to lead to reinnervation by sprouting (Garrett 1966*a*,*b*; Ekström & Emmelin 1974*a*,*b*), and the sublingual gland secretes spontaneously even after denervation (Emmelin 1953).

Secretory inactivity leads to autophagy of secretory granules (Hand & Ball 1988), and secretory material appears to be a component of the microliths in submandibular acinar cells, which are present in autophagosomes (Triantafyllou 1991). Almost all of these microliths are in central acinar cells and contain crystals of hydroxyapatite (Triantafyllou 1991). The secretory granules of these cells appear to contain a large amount of sequestered calcium (Verdugo *et al.* 1987; Triantafyllou 1991) that would be released in an ionized form during degeneration of secretory granules and be available to precipitate on to debris and so produce calcified microliths in the autophagosomes. This is possibly a physiological process to safeguard the cell from poisoning by

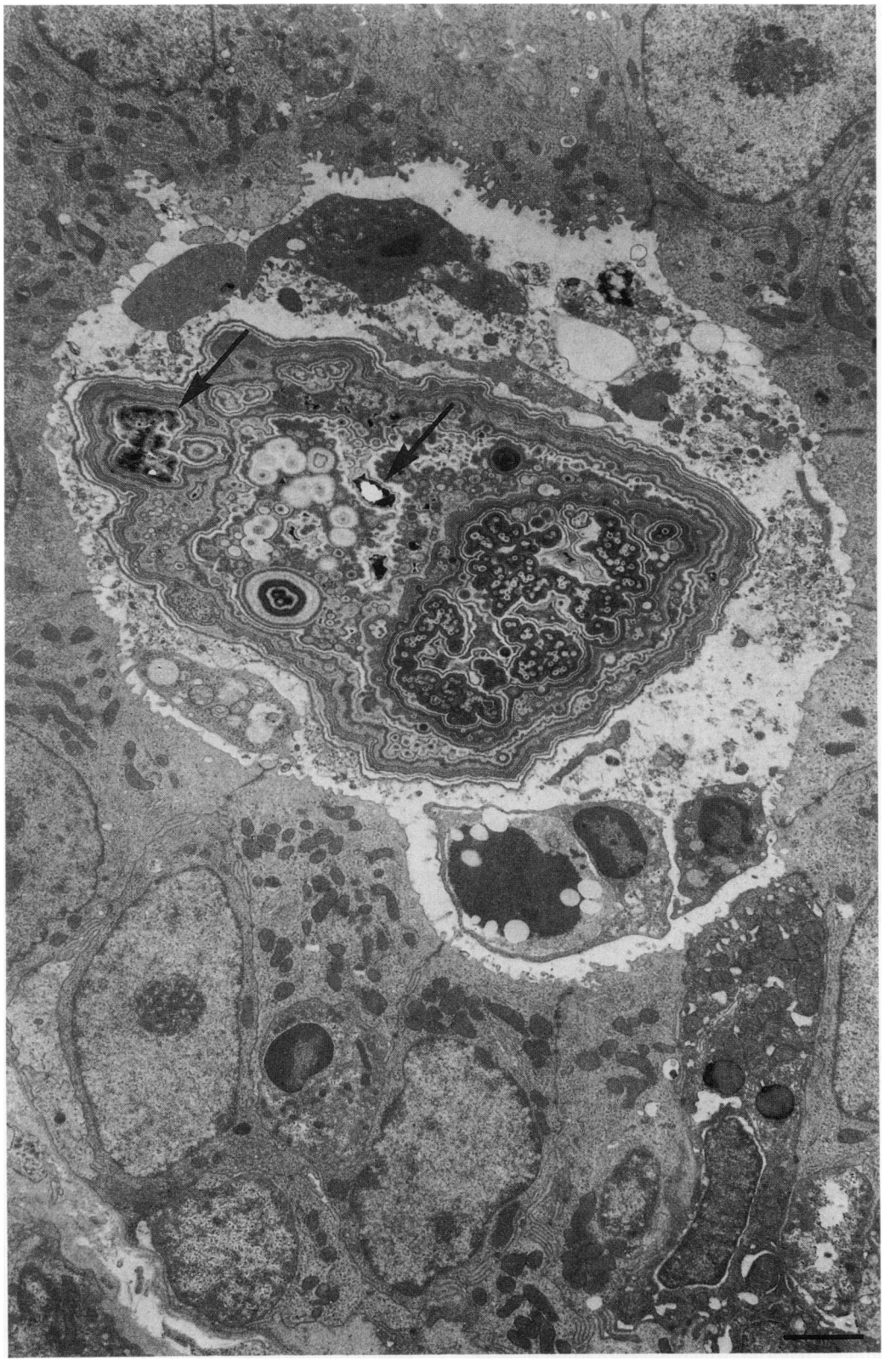

Figure 4. Submandibular gland 24 days after parasympathectomy and sympathetically stimulated. Immersion fixed in glutaraldehyde and formaldehyde, and subsequently in osmium tetroxide. A microlith present in the lumen of a large intralobular duct consists of lamellae variously arranged around single cores, groups of cores, and groups of lamellae, which indicates that many small microliths had accreted to form this large microlith. The lamellae and most of the cores consist of concentrated granular material, and a few cores consist of concentrated crystals (arrows). Secretory material, cellular debris and neutrophils are present in the lumen, and neutrophils between ductal cells. × 6100; bar 2 μm.

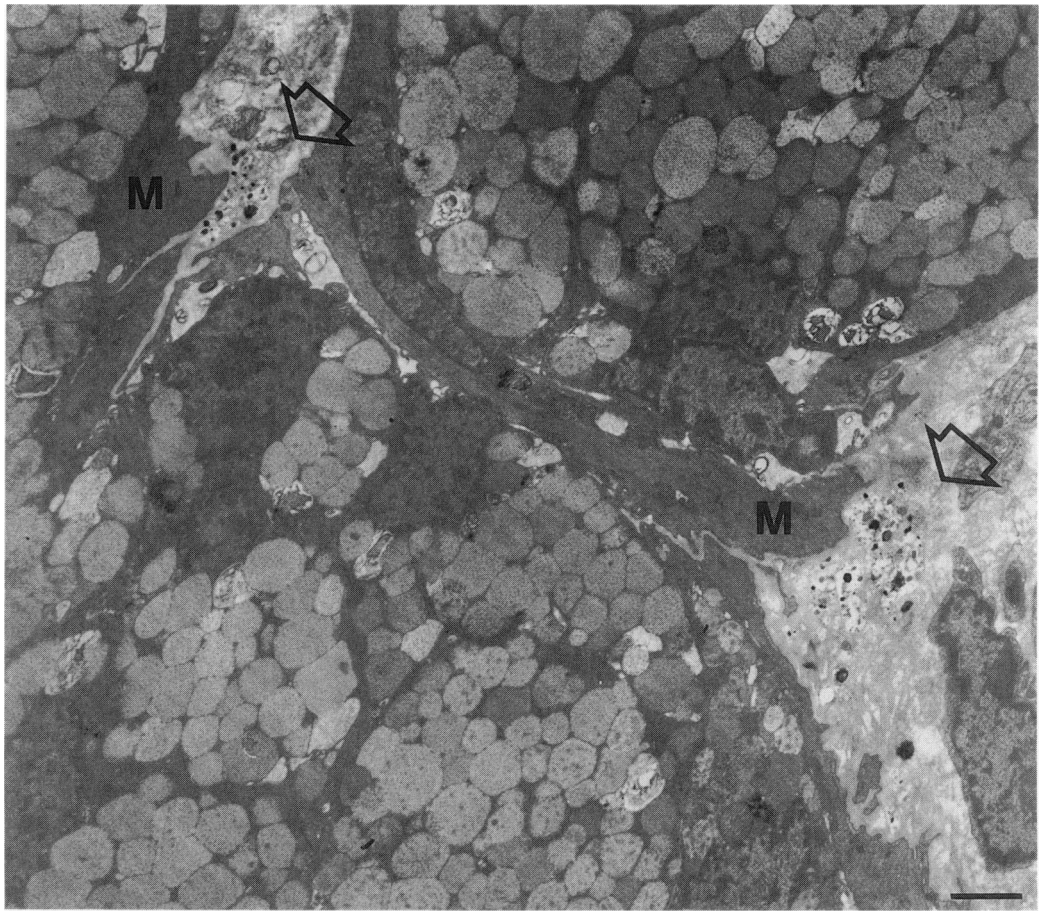

Figure 5. Submandibular gland 22 days after parasympathectomy and sympathetically stimulated. Immersion fixed in glutaraldehyde and formaldehyde, and subsequently in osmium tetroxide. Two groups of microliths (arrows) are situated in the thickened basement membrane that overlies processes of myoepithelial cells (M) that protrude into the stroma. × 4500; bar 2 μm.

overwhelming increases of intracellular ionized calcium (S.Y. Ali 1991, personal communication).

The microliths in ductal cells could arise during autophagy of redundant cellular material during atrophy (Garrett & Kidd 1975; Uddin 1989) or be endocytosed from lumina (Lotti & Hand 1989).

The microliths in ductal lumina are the most numerous and appear to be the first to be formed. They possibly arise from secretory material and cellular debris that stagnate in lumina in the absence of flushing produced by parasympathetic stimulation (Garrett & Kidd 1975). The finding that many of these microliths consist essentially of granular material, which appears to be organic and formed by inspissation of secretory material (Triantafyllou 1991), suggests that possibly there is insufficient calcium in ductal lumina to produce highly calcified microliths.

Macrophages have been found to be important scavengers in salivary glands (Harrison & Garrett 1976), and the finding of microliths in macrophages in the parenchyma and lumina suggests that they are important scavengers of microliths.

The numerous small microliths in the basement membrane overlying protruding processes of myoepithelial cells possibly arise from vesicles that are released into the stroma by budding off from the cell membrane of the myoepithelial cells, which contains alkaline phosphatase (Davies & Garrett 1972), and are thus similar to matrix vesicles that are important in the initiation of calcification (Ali 1983; Varma & Kim 1985; Ghadially 1988; Rees & Ali 1988; Anderson 1989). Such microliths may be protected from scavenging macrophages by the enveloping basement membrane and persist (Varma & Kim 1985).

Figure 6. Submandibular gland 24 days after parasympathectomy and sympathetically stimulated. Perfusion fixed in glutaraldehyde and formaldehyde, and subsequently immersion fixed in osmium tetroxide. A macrophage in the parenchyma of a large intralobular duct contains a large phagosome in which is a microlith, debris, and electron-lucent granular material of similar appearance to the secretory material in the lumen. The microlith consists of granular material variously concentrated to form cores and lamellae. × 6100; bar 2 μm.

The occurrence of microliths in most of the parasympathectomized submandibular glands is similar to the human condition, in which microliths are present in most submandibular glands (Epivatianos & Harrison 1989). This suggests that secretory inactivity in the human submandibular gland may be an aetiological factor of microlithiasis and thereby of chronic sialadenitis and sialolithiasis.

Acknowledgements

We gratefully acknowledge the technical assistance of Mr R.H. Hartley and Miss Katherine L. Paterson.

References

ALI S.Y. (1983) Calcification of cartilage. In *Cartilage*. Vol.1: *Structure, Function and Biochemistry*. Ed. B.K.Hall. New York, London: Academic. pp. 343–378.

ANDERSON H.C. (1989) Mechanism of mineral formation in bone. *Lab. Invest.* **60,** 320–330.

BAILEY N.T.J. (1981) *Statistical Methods in Biology*, Second edition. London, New York, Melbourne, Auckland: Edward Arnold. pp. 52–66.

DAVIES K.J. & GARRETT J.R. (1972) Improved preservation of alkaline phosphatase in salivary glands of cat. *Histochem. J.* **4,** 365–379.

EDWARDS A.V. & GARRETT J.R. (1988) Submandibular responses to stimulation of the sympathetic innervation following parasympathetic denervation in cats. *J. Physiol.* **397,** 421–431.

EKSTRÖM J. & EMMELIN N. (1974a) Reinnervation of the denervated parotid gland of the cat. *Q. J. Exp. Physiol.* **59,** 1–9.

EKSTRÖM J. & EMMELIN N. (1974b) The secretory innervation of the parotid gland of the cat: an unexpected component. *Q. J. Exp. Physiol.* **59,** 11–17.

EMMELIN N. (1953) On spontaneous secretion of saliva. *Acta Physiol. Scand.* (**Suppl. III**) 34–58.

EMMELIN N. & GARRETT J.R. (1989) Nerve-induced secretion of parotid acinar granules in cats. *Cell Tissue Res.* **257,** 549–554.

EPIVATIANOS A. & HARRISON J.D. (1989) The presence of microcalculi in normal human submandibular and parotid salivary glands. *Archs Oral Biol* **34,** 261–265.

EPIVATIANOS A., HARRISON J.D., GARRETT J.R., DAVIES K.J. & SENKUS R. (1986) Ultrastructural and histochemical observations on intracellular and luminal microcalculi in the feline sublingual salivary gland. *J. Oral Path.* **15,** 513–517.

EPIVATIANOS A., HARRISON J.D. & DIMITRIOU T. (1987) Ultrastructural and histochemical observations on microcalculi in chronic submandibular sialadenitis. *J. Oral Path.* **16,** 514–517.

GARRETT J.R. (1966a) The innervation of salivary glands. III. The effects of certain experimental procedures on cholinesterase-positive nerves in glands of the cat. *J.R. Microsc. Soc.* **86,** 1–13.

GARRETT J.R. (1966b) The innervation of salivary glands. IV. The effects of certain experimental procedures on the ultrastructure of nerves in glands of the cat. *J.R.Microsc.Soc.* **86,** 15–31.

GARRETT J.R. & KIDD A. (1975) Effects of nerve stimulation and denervation on secretory material in submandibular striated duct cells of cats, and the possible role of these cells in the secretion of salivary kallikrein. *Cell Tissue Res.* **161,** 71–84.

GHADIALLY F.N. (1988) *Ultrastructural Pathology of the Cell and Matrix*. Third edition. London: Butterworths. pp. 1080–1085, 1278–1289.

HAND A.R. & BALL W.D. (1988) Ultrastructural immunocytochemical localization of secretory proteins in auutophagic vacuoles of parotid acinar cells of starved rats. *J. Oral Path.* **17,** 279–286.

HARRISON J.D. & EPIVATIANOS A. (1992) Production of microliths and sialadenitis in rats by a short combined course of isoprenaline and calcium gluconate. *Oral Surg.* **73,** 585–590.

HARRISON J.D. & GARRETT J.R. (1976) Inflammatory cells in duct-ligated salivary glands of the cat: a histochemical study. *J. Path.* **120,** 115–119.

HUMPHREY C.D. & PITTMAN F.E. (1974) A simple methylene blue-azure II-basic fuchsin stain for epoxy-embedded tissue sections. *Stain Technol.* **49,** 9–14.

KÖNIG B. & KÜHNEL W. (1986) Licht- und elektronenmikroskopische Untersuchungen an der Glandula parotis und der Glandula submandibularis der Hauskatze. *Z. Mikr.-Anat. Forsch.* **100,** 469–483.

LILLIE R.D. (1965) *Histopathologic Technic and Practical Histochemistry*, Third edition. New York, Toronto, Sydney, London: McGraw-Hill. pp. 32–60.

LOTTI L.V. & HAND A.R. (1989) Endocytosis of native and glycosylated bovine serum albumin by duct cells of the rat parotid gland. *Cell Tissue Res.* **255,** 333–342.

REES J.A. & ALI S.Y. (1988) Ultrastructural localisation of alkaline phosphatase activity in osteoarthritic human articular cartilage. *Ann. Rheum. Dis.* **47,** 747–753.

REYNOLDS E.S. (1963) The use of lead citrate at high pH as an electron-opaque stain in electron microscopy. *J. Cell Biol.* **17,** 208–212.

SCOTT J. (1978) The prevalence of consolidated salivary deposits in the small ducts of human submandibular glands. *J. Oral Path.* **7,** 28–37.

SHACKLEFORD J.M. & WILBORN W.H. (1970) Ultrastructural aspects of cat submandibular glands. *J. Morph.* **131,** 253–275.

SEIFERT G. & DONATH K. (1977) Zur Pathogenese des Küttner-Tumors der Submandibularis. Analyse von 349 Fällen mit chronischer Sialadenitis der Submandibularis. *H.N.O. (Berl.)* **25,** 81–92.

TANDLER B. (1965) Electron microscopical observations on early sialoliths in a human submaxillary gland. *Archs Oral Biol.* **10,** 509–522.

TANDLER B. & POULSEN J.H. (1977) Ultrastructure of the cat sublingual gland. *Anat. Rec.* **187,** 153–171.

TRIANTAFYLLOU A. (1991) Microlithiasis of the major salivary glands of cat: a morphological, histochemical and biochemical study. PhD. Thesis, University of London.

UDDIN M. (1989) Autonomic denervation effects on the kallikrein and striated duct cells of the rat and cat submandibular glands. *Anat. Anz.* **169,** 273–284.

VARMA V.A. & KIM K.M. (1985) Placental calcification: ultrastructural and X-ray microanalytic studies. *Scan. Electron Micr.* **4,** 1567–1572.

VERDUGO P., DEYRUP-OLSEN I., AITKEN M., VILLALON M. & JOHNSON D. (1987) Molecular mechanism of mucin secretion. I The role of intragranular charge shielding. *J. Dent. Res.* **66,** 506–508.